

## Fe implantation effect in the 6H-SiC semiconductor investigated by Mössbauer spectrometry

M.L. Diallo, L. Diallo, A. Fnidiki, L. Lechevallier, F. Cuvilly, I. Blum, M. Viret, M. Marteau, D. Eyidi, J. Juraszek, et al.

► **To cite this version:**

M.L. Diallo, L. Diallo, A. Fnidiki, L. Lechevallier, F. Cuvilly, et al.. Fe implantation effect in the 6H-SiC semiconductor investigated by Mössbauer spectrometry. *Journal of Applied Physics, American Institute of Physics*, 2017, 122, pp.083905. <10.1063/1.4992102>. <cea-01591469>

**HAL Id: cea-01591469**

**<https://hal-cea.archives-ouvertes.fr/cea-01591469>**

Submitted on 21 Sep 2017

**HAL** is a multi-disciplinary open access archive for the deposit and dissemination of scientific research documents, whether they are published or not. The documents may come from teaching and research institutions in France or abroad, or from public or private research centers.

L'archive ouverte pluridisciplinaire **HAL**, est destinée au dépôt et à la diffusion de documents scientifiques de niveau recherche, publiés ou non, émanant des établissements d'enseignement et de recherche français ou étrangers, des laboratoires publics ou privés.

## Fe implantation effect in the 6H-SiC semiconductor investigated by Mössbauer spectrometry

M. L. Diallo,<sup>1</sup> L. Diallo,<sup>1</sup> A. Fnidiki,<sup>1,a)</sup> L. Lechevallier,<sup>1,2</sup> F. Cuvilly,<sup>1</sup> I. Blum,<sup>1</sup> M. Viret,<sup>3</sup> M. Marteau,<sup>4</sup> D. Eyidi,<sup>4</sup> J. Juraszek,<sup>1</sup> and A. Declémy<sup>4</sup>

<sup>1</sup>Normandie Univ., INSA Rouen, UNIROUEN, CNRS, GPM, 76800 Rouen, France

<sup>2</sup>Département de GEH, Université de Cergy-Pontoise, rue d'Eragny, Neuville sur Oise, 95031 Cergy-Pontoise, France

<sup>3</sup>Service de Physique de l'Etat Condensé (DSM/IRAMIS/SPEC), UMR 3680 CNRS, Bât. 772, Orme des Merisiers, CEA Saclay, 91191 Gif sur Yvette, France

<sup>4</sup>Institut PPRIME, UPR 3346 CNRS, Université de Poitiers, ENSMA, SP2MI, Téléport 2, 11 Bvd M. et P. Curie, 86962 Futuroscope, Chasseneuil, France

(Received 26 June 2017; accepted 10 August 2017; published online 24 August 2017)

P-doped 6H-SiC substrates were implanted with <sup>57</sup>Fe ions at 380 °C or 550 °C to produce a diluted magnetic semiconductor with an Fe homogeneous concentration of about 100 nm thickness. The magnetic properties were studied with <sup>57</sup>Fe Conversion Electron Mössbauer Spectrometry at room temperature (RT). Results obtained by this technique on annealed samples prove that ferromagnetism in <sup>57</sup>Fe-implanted SiC for Fe concentrations close to 2% and 4% is mostly due to Fe atoms diluted in the matrix. In contrast, for Fe concentrations close to 6%, it also comes from Fe in magnetic phase nano-clusters. This study allows quantifying the Fe amount in the interstitial and substitutional sites and the nanoparticles and shows that the majority of the diluted Fe atoms are substituted on Si sites inducing ferromagnetism up to RT. *Published by AIP Publishing.*

[<http://dx.doi.org/10.1063/1.4992102>]

### I. INTRODUCTION

Exploiting the spin in addition to the charge of the electron provides new functionality to microelectronic devices. In order to produce magnetic materials with highly spin-polarized electrons, many efforts have been concentrated on the preparation of diluted magnetic semiconductors (DMSs) doped with transition metals.<sup>1</sup> Indeed, doping a semiconductor with a 3d magnetic element (Cr, Mn, Fe, and Co) confers ferromagnetic (FM) properties, while keeping the semiconductor nature of the material. The discovery of DMSs with relatively high Curie temperatures, such as (In, Mn) As,<sup>2</sup> and especially (Ga, Mn) As,<sup>3</sup> initiated a major international research effort during the last two decades, in order to understand the origin and the mechanism of the magnetic properties of this type of materials. Many advances have been made in the growth and annealing of these samples in order to minimize the presence of secondary phases or compensating defects which are detrimental to the desired properties. (In, Mn) As showed ferromagnetic properties because Mn is an acceptor in an III-V semiconductor which induces ferromagnetism through the holes. The archetype of these DMSs is the (Ga, Mn) As which has certainly been the more extensively studied and holds the highest Curie temperature record, 60 K by Ohno *et al.*,<sup>3</sup> 110 K still by Matsukura *et al.*<sup>4</sup> and finally 160 K in tri-layers of (Ga, Mn) As/GaAs/(Ga, Mn) As.<sup>5</sup> Indeed the (Ga, Mn) As has the highest Curie temperature, of the order of 180 K,<sup>6</sup> among all the III-V systems abundantly studied. This is a major step forward but the

emergence of a candidate with a ferromagnetic order at room temperature, or even beyond, is still expected. A possibility to achieve the T<sub>C</sub> values higher than 300 K was forecasted for certain wide-gap DMSs with rather a high concentration of free holes.<sup>7</sup> This prognosis gave impetus a great deal of experiments aimed at the founding of DMS materials with high T<sub>C</sub>. Many authors reported that they observed ferromagnetism in the corresponding objects at temperatures above room one. However, most of these observations later turned out to be the consequence of the presence of precipitates in the studied specimens or inclusions of other phases of transition metal (TM) compounds in solid solutions, to which the DMS specimens belong.<sup>8</sup> This circumstance stimulated the appearance of theoretical works, where the ferromagnetic ordering in such specimens was explained apart from the exchange interaction between charge carriers and doping magnetic ions.<sup>9</sup> Numerous works have been carried out in order to produce materials with a Curie temperature above the room temperature. But, after more than a decade of intense research in DMSs, no Curie temperature higher than the room temperature has been obtained. Moreover, the nature and origin of ferromagnetism in III-V compounds remain controversial.<sup>10</sup> A little attention has been paid so far for the wide band gap semiconductor silicon carbide (gap energy E<sub>g</sub> = 3.0 eV for 6H-SiC) thanks to its large potential for high-power and high-temperature electronics devices and its excellent transport properties. Theodoropoulou *et al.* showed that 5% of Fe atoms implanted in the 6H-SiC polytype lead to a ferromagnetic material at a temperature of about 250 K.<sup>11</sup> No secondary phase was detected in their samples. Similar findings have been reported by Pearton *et al.*<sup>12</sup> and Stromberg *et al.*<sup>13</sup> Indeed, these authors carried

<sup>a)</sup>Author to whom correspondence should be addressed: abdeslem.fnidiki@univ-rouen.fr

out an in-depth study in the 6H-SiC system implanted with different Fe doses. They found a DMS behavior for Fe concentrations of less than 3%. The magnetic response appears to come mainly from Fe<sub>3</sub>Si phase nanoparticles. Similar conclusions have also been reported by Dupeyrat *et al.* and Diallo *et al.* on the Fe-doped 6H-SiC.<sup>14–16</sup> The formation of nano-sized particles of nano-metric size is partly responsible for the magnetic properties observed on their samples after annealing.

The present work reports on the structural and magnetic behavior of <sup>57</sup>Fe-doped 6H-SiC samples. <sup>57</sup>Fe Conversion Electron Mössbauer Spectrometry (CEMS) was employed for the study of the local environment of the <sup>57</sup>Fe nucleus in the SiC matrix. This technique allowed us to determine the structural modifications of our samples, after the implantation and the different annealing and notably the amount of Fe atoms at the substitutional and interstitial sites. It also allowed for the determination of the paramagnetic and ferromagnetic components of each sample. So, it will be shown that the Si atoms substitution by the Fe atoms in the Si-sites of the 6H-SiC lattice is the main source of ferromagnetism in Fe-implanted 6H-SiC.

## II. EXPERIMENTAL

6H-SiC substrates from commercial (CREE) near (0001)-oriented with an uppermost epitaxial layer 200 nm thick of p-type ( $n_A - n_D \sim 10^{+20} \text{ Al/cm}^3$ ) were co-implanted with 30 to 160 keV <sup>56</sup>Fe<sup>+</sup> and <sup>57</sup>Fe<sup>+</sup> ions (in respective 2/3–1/3 ratio) at doses  $10^{+16} \text{ /cm}^2$  leading to an Fe concentration of about 2, 4, and 6 at. % at depth between 20 and 100 nm from the sample surface, which was verified by Rutherford Backscattering Spectrometry (RBS) at the CSNSM-Orsay (Centre de Sciences Nucléaires et de Sciences de la Matière).<sup>14,17</sup> The samples were held at 380 and 550 °C during implantation in order to avoid amorphisation.<sup>18</sup> After the implantation, the 6 at. % Fe samples were subjected to a rapid thermal annealing at 900 and 1300 °C for 4 min. The 4 at. % Fe samples were annealed at 1000 °C for 85 min. The 2 at. % Fe samples were subjected to a rapid thermal annealing at 1300 °C for 4 min. The CEMS technique has a penetration depth of about 80–100 nm compared to the overall thickness of the samples (400 μm) and is useful for analyzing the near surface region<sup>19,20</sup> of the implanted samples studied in this work. CEMS experiments are performed at room temperature (RT) by using a constant acceleration set-up in reflection geometry and a <sup>57</sup>Co source diffused into the rhodium matrix. CEMS spectra were fitted by using the four components of the Gunnlaugsson model.<sup>21</sup> The single Fei (C) and Fei (Si) lines are assigned to the interstitial sites of Fe atoms surrounded by four C or Si atoms, respectively. The Fs fraction corresponds to the positioning of the substitutional Fe atoms in C or Si sites. The Fd fraction, unlike the three other components, is attributed to Fe atoms located in strongly disturbed zones, often called “amorphous state,” which result from the damage caused during the implantation. This Fd fraction is fitted by a doublet. Velocities and isomer shifts are given relative to α-Fe at RT.

## III. RESULTS AND DISCUSSION

### A. 380 °C implanted samples with 4 at. % Fe

CEMS spectra obtained on the as-implanted sample and the 1000 °C annealed sample are shown in Figs. 1(a) and 1(b), respectively. The spectrum in Fig. 1(a) is fitted between –2 and +2 mm/s and the one in Fig. 1(b) is fitted between –10 and +10 mm/s. This is due to the fact that the spectrum of the as implanted sample is characteristic of an entirely paramagnetic sample, whereas the one in the 1000 °C annealed sample contains a magnetic component which extends between –10 mm/s and +10 mm/s. The corresponding Mössbauer spectra parameters for these two samples are presented in Table I. In these two samples, the most important contribution to the Mössbauer spectra is the paramagnetic contribution. This component represents 100% of the whole spectrum for the as implanted sample and 74% for annealed sample which also contains a magnetic component (26% of the total area of the spectrum).

Gunnlaugsson results showed that the Fei (Si) component is much lower than the Fei (C) component and disappears above 600 °C.<sup>21</sup> As the samples were implanted at 380 °C (or 550 °C) and annealed at 1000 °C (or 900 and 1300 °C), this component was not taken into account in the fits in order to limit the number of parameters. The Fs component is relative to the Fe atoms diluted in the SiC matrix entering the Si or C atom sites, without distinction. It has been shown that Fe diluted in the SiC matrix is either in interstitial sites or in Si substitution sites (only, and not in C substitution sites)<sup>9,23,24</sup> where it is then ferromagnetic<sup>24</sup> or ferromagnetic and paramagnetic.<sup>9,22</sup> The paramagnetic Fs component is then represented by a singlet [denoted by Fs (para)] and the ferromagnetic Fs component by a sextet [denoted by Fs (ferro)]. The sum of the Fei (C) and Fs (para) components corresponds to a part of the totality of the paramagnetic component of the Mössbauer spectra. The fit of the spectra was carried out by introducing the values given by Gunnlaugsson for the isomer shift. The optimization of the values of these parameters allowed reproducing the experimental spectra. The Mössbauer spectrum of the as-implanted sample was fitted using two Fs (para) and Fei (C) singlets and one Fd doublet. For this sample, the main component (75.7% of the spectrum) is the Fd component which corresponds to “amorphous” areas caused by the implantation. Thus, in the as-implanted state, the environment around the Fe atoms is highly disturbed and characterizes the inhomogeneity of the microstructure. Fs (para) and Fei (C) components are much smaller than the Fd component and respectively correspond to 16.6 and 7.7% of the total area of the spectrum. The Mössbauer spectrum of the 1000 °C annealed sample is shown in Fig. 1(b). Above this temperature, the Fd component attributed to the “amorphous” zones completely disappeared indicating a restoration of the crystalline structure of the material, as also shown by the XRD.<sup>16</sup> This spectrum could be fitted using the Fs (para) and Fei (C) singlets characteristic of the paramagnetic contribution but also with a sextuplet, characteristic of the Fs (ferro) ferromagnetic contribution. This Fs (ferro) component (ferromagnetic) is due to the Fe atoms diluted in the SiC matrix and substituted to the

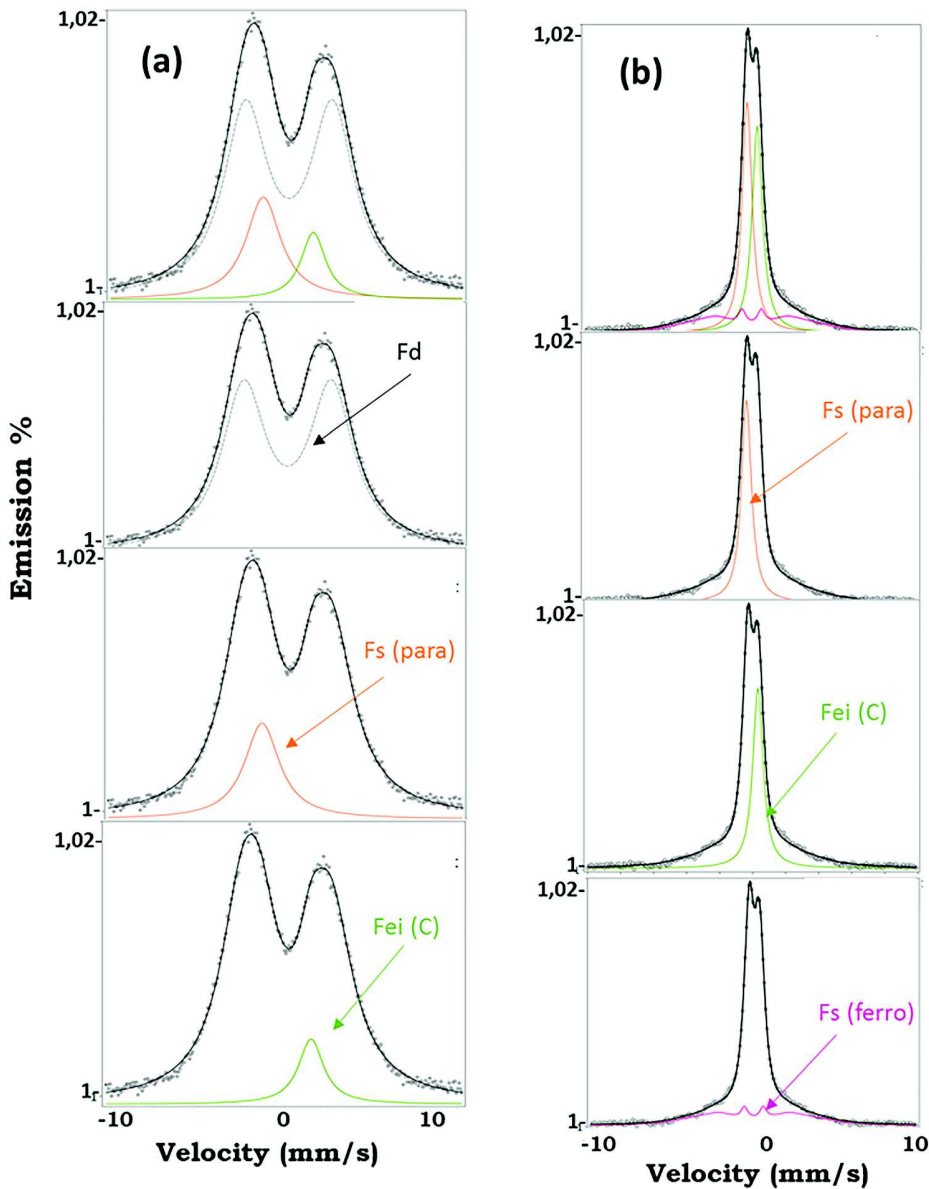


FIG. 1. Mössbauer spectra of the samples implanted at 380°C with 4 at. % Fe (a) as-implanted, (b) annealed at 1000°C.

Si atoms. Indeed, unpublished atomic probe tomography (APT) results<sup>25</sup> show that in this sample, Fe atoms are divided into iron-rich nano-particles (non-magnetic definite phases) (10% Fe) and homogeneously distributed diluted Fe atoms (90% Fe). Taking into account previously published results of SQUID measurements,<sup>16</sup> supposing that all the observed magnetization comes from nano-particles leads to an unrealistic

TABLE I. Mössbauer parameters used to fit samples implanted at 380°C with 4 at. % Fe.

Samples	Components	$\delta$ (mm/s)	QS (mm/s)	$B_{\text{hf}}$ (kOe)	Relative area (%)
As-implanted	Fd	0.140	1.014		75.7
	Fs (para)	-0.160	0		16.6
	Fei (C)	0.423	0		7.7
Annealed 1000°C	Fs (para)	-0.146	0		37.9
	Fei (C)	0.462	0		35.5
	Fs (ferro)	0.131	0	225.3	26.6

value of the magnetic moment per Fe atom in nano-particles (about  $10 \mu_B/\text{Fe}$  at 250 K). As a consequence, diluted Fe atoms have to strongly contribute to the observed magnetization. On an other hand, it has been shown that only diluted Fe atoms substituted at the Si-site can carry a non-zero magnetic moment,<sup>9,24</sup> and then these Fe atoms correspond to the  $F_s$  (ferro) component (ferromagnetic) of the observed Mössbauer spectrum. An increase of the fraction of substituted Fe atoms  $F_s$  (para) and the fraction of Fe atoms in interstitial sites  $\text{Fei (C)}$  is observed. They respectively represent 37.9% and 35.5% for the  $F_s$  (para) and  $\text{Fei (C)}$  components of the whole area of the spectrum. The sum of these two components is less than 100%. Indeed, on the Mössbauer spectrum, a sextuplet appears which reflects the appearance of a non-negligible ferromagnetic contribution (26.6%), the  $F_s$  (ferro) magnetic contribution.

## B. 550°C implanted samples with 6 at. % Fe

In order to observe the effects of both the increase of the implanted Fe amount and the increase of the implantation

temperature on the 6H-SiC structural and magnetic properties, the Fe amount has been increased from 4 to 6 at. % and the implantation temperature is gone from 380 °C to 550 °C.

Figure 2 shows the Mössbauer spectra obtained at room temperature for the as-implanted sample and the 900 and 1300 °C annealed samples, respectively. As was showed in a previous study, the as-implanted sample is totally paramagnetic and the spectrum has been fitted with only two components, the Fei (C) interstitial and the Fs (para) substitutional components. Indeed, it has been showed by Gunnlaugsson *et al.* that the Fd fraction component corresponding to the damaged sites disappears when the sample was held at high temperature (above to 900 °C).<sup>21</sup> In our study, the implantation at 550 °C is sufficient to eliminate this component characteristic of a disturbed structure and to restore the crystalline structure of the material to a large extent. As

shown in Fig. 2(a) for the as-implanted sample, the two Fs (para) and Fei (C) components contained in this spectrum indicate that 53% of Fe atoms are located in the substituted sites and 47% in interstitial sites. These two components are of the same order of magnitude. After annealing at 900 and 1300 °C [Figs. 2(b) and 2(c)], the Fei (C) and Fs (para) components remain, but three magnetic components, which are represented by sextets, are added. The first magnetic component is what we called the Fs (ferro) component, considered as the magnetic fraction due to the Fe atoms diluted in the SiC matrix. The two other components are attributed to magnetic phases and mainly to the Fe<sub>3</sub>Si phase which are contained in nanoclusters, as already observed.<sup>15</sup> Table II shows the parameters used to fit the Mössbauer spectra of the 550 °C implanted samples. After annealing at 900 °C [Fig. 2(b)], only one magnetic component appears additional to

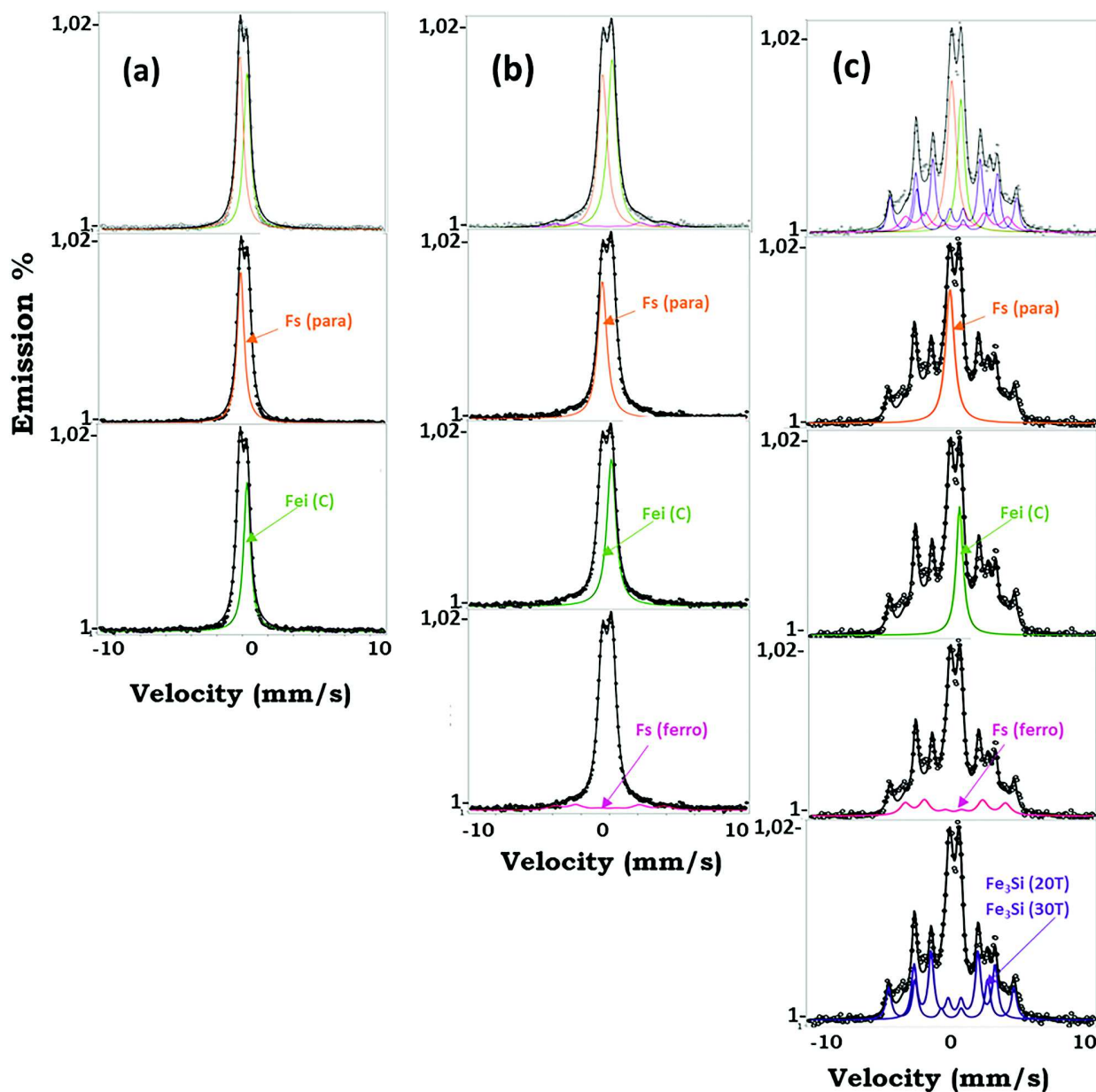


FIG. 2. Mössbauer spectra of the samples implanted at 550 °C with 6 at. % Fe. (a) as-implanted, (b) annealed at 900 °C, and (c) annealed at 1300 °C.



TABLE II. Mössbauer parameters used to fit as-implanted sample and annealed at 900 and 1300 °C samples implanted at 550 °C with 6 at. % Fe.

Samples	Components	$\delta$ (mm/s)	$B_{hf}$ (kOe)	Relative area (%)
As-implanted	Fs (para)	-0.056		53.0
	Fei (C)	0.506		47.0
900 °C	Fs (para)	-0.353		43.4
	Fei (C)	0.302		47.3
	Fs (ferro)	0.086	240	9.3
Annealed 1300 °C	Fs (para)	-0.034		24.1
	Fei (C)	0.675		16.5
	Fs (ferro)	0.270	246	14.0
	Fe <sub>3</sub> Si	0.345	196	28.3
		0.059	304	17.1

the paramagnetic doublet. It is the Fs (ferro) magnetic component. This low contribution (9.3%) is attributed to the ferromagnetic behavior of this sample but is greatly reduced nevertheless. It corresponds to the Fe atoms diluted in the matrix because for this annealing, the sample contains an amount of nano-particles (not or slightly ferromagnetic) that is too small, which cannot explain the magnetism of this sample.<sup>15</sup> The Fs (para) and Fei (C) fractions represent approximately 43% and 47% of the whole area of the spectrum. The Fs (para) fraction is slightly reduced for the 900 °C annealed sample compared to the as-implanted sample. It can be explained by the fact that the Fe atoms fraction increases in the magnetic Si- sites (Fs (ferro) component) at the expense of other sites due to the increase of the annealing temperature.

After the 1300 °C annealing [Fig. 2(c)], the magnetic contributions become more significant on the Mössbauer spectrum. Therefore, the 1300 °C annealed sample was fitted as the sum of three ferromagnetic sextets (two for the Fe<sub>3</sub>Si magnetic phase and one for the Fs (ferro) magnetic contribution due to diluted Fe) and two Fs (para) and Fei (C) paramagnetic components. The fit results indicate that approximately 60% of this spectrum can be fitted with the magnetic components. Increasing the annealing temperature of the sample from 900 °C to 1300 °C allowed increasing the ferromagnetic fraction from 10% to 60%, approximately. This increase is mainly due to the emergency of the Fe<sub>3</sub>Si phase that is known in the literature to be ferromagnetic, as mentioned above. Moreover, this Fe<sub>3</sub>Si phase is contained in the biggest nanoparticles included in this sample, as showed in Ref. 15. The magnetic components due to this phase represent (28.3 + 17.1 = 45.4) of the whole area of this spectrum when the Fs (ferro) component only represents 14%. So, the Fs (ferro) component only approximately represents one third of the magnetic components of this sample. The increase of the magnetic part of this sample with the increase of the annealing temperature is due to the formation of big magnetic nanoparticles but not the increase of the magnetism due to the diluted part of the Fe atoms characterized by the Fs (ferro) component, which is the objective of a DMS.

Figure 3 shows the evolution of Fe fractions attributed to the substitutional and interstitial sites versus temperature deduced from the Mössbauer study for samples implanted at 380 and 550 °C containing 4 and 6 at. % Fe.

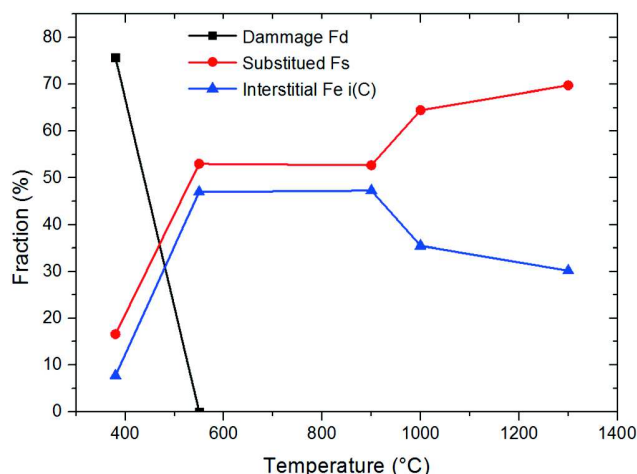


FIG. 3. Evolution of the Fe atoms fractions in the substitutional and interstitial sites versus temperature.

As shown in this figure, we can first observe an important fraction Fd (~75%) for 380 °C. This component is attributed to Fe atoms located in small “amorphous” pockets, as explained above. It disappears at 550 °C (as observed above) due to the matrix structure restoration. The substitutional and interstitial Fe atoms fractions increase with the increase of the implantation temperature (from 380 °C to 550 °C) due to the complete disappearing of the Fd component. Consequently, Fs (para) increases up to 53% at 550 °C compared to 16.6% for the 380 °C implantation temperature. The same evolution is observed for the Fei (C) fraction which increases from 7.7% for the 380 °C implantation temperature to 47% for the 550 °C implantation temperature. Between 550 and 900 °C, there is only a slight evolution of the two Fei (C) and Fs (para) fractions. On the other hand, above 900 °C, there is a significant evolution of the Fe atoms fractions in the substitutional and interstitial sites. These two fractions evolve in the opposite direction. The increase of the annealing temperature above 900 °C results in an increase of the fraction of Fe atoms in substitution sites and consequently in a decrease of the fraction of Fe atoms in interstitial sites. Thus, the Fs (para) and Fei (C) fractions are respectively 64.5% and 35.5% for the 1000 °C annealing and 69.7% and 30.2% for the 1300 °C annealing. The annealing at high temperatures (1000 and 1300 °C) gives preferential displacement of Fe atoms in the substitution sites rather than in interstitial sites. This behavior has to be seen as the result of the Si vacancies mobility which is lying in this temperature range around 750 °C in SiC.<sup>26</sup>

### C. 380 °C implanted samples with 2 at. % Fe

We saw in the previous paragraph that the increase of the implanted Fe amount in SiC and the increase of the annealing temperature lead to magnetic samples but also to the presence of Fe-Si based nanoparticles (not showed here) for which the core phases are often magnetic. It is then difficult to separate the magnetism due to Fe atoms diluted in the matrix from the magnetism due to Fe atoms contained in magnetic nanoparticles. To avoid this problem while

maintaining the magnetism of samples, we decreased the Fe amount implanted in the SiC samples up to 2 at. %. The samples were implanted at 380 °C rather 550 °C in order to minimize the nanoparticle amount.

CEMS spectra obtained on the as-implanted sample and on the 1300 °C annealed sample are shown in Fig. 4. These spectra were fitted as previously according to the same model,<sup>21</sup> starting with the as-implanted sample which is totally paramagnetic and continuing with the 1300 °C annealed sample. The spectrum of the as-implanted sample [Fig. 4(a)] is fitted using two Fs (para) and Fei (C) singlets and the Fd component which corresponds to “amorphous” zones, as already seen above.<sup>21</sup> The different Mössbauer components indicate that 82% of Fe atoms are in “amorphous”

zones, 13% in substituted sites and 5% in interstitial sites, respectively. This leads to a paramagnetic state. It corresponds to Fe atoms in non-magnetic environments. It may also be characteristic of a superparamagnetic state. Indeed, if Fe atoms are located in magnetic zones, or in nanoparticles with high Fe content but very small sizes (a few nm or less), magnetically isolated the ones from another, a relaxation of the moments occurs leading to a paramagnetic total behavior of the sample. However, a study in tomographic atomic probe performed on these samples (but not showed here) did not reveal the presence of nanoparticles, even with a size less than 1 nm. Thus, the Fe atom distribution in this sample is homogeneous. For the fit of the 1300 °C annealed sample, the Fs (para) singlet and the Fei (C) singlet were retained as

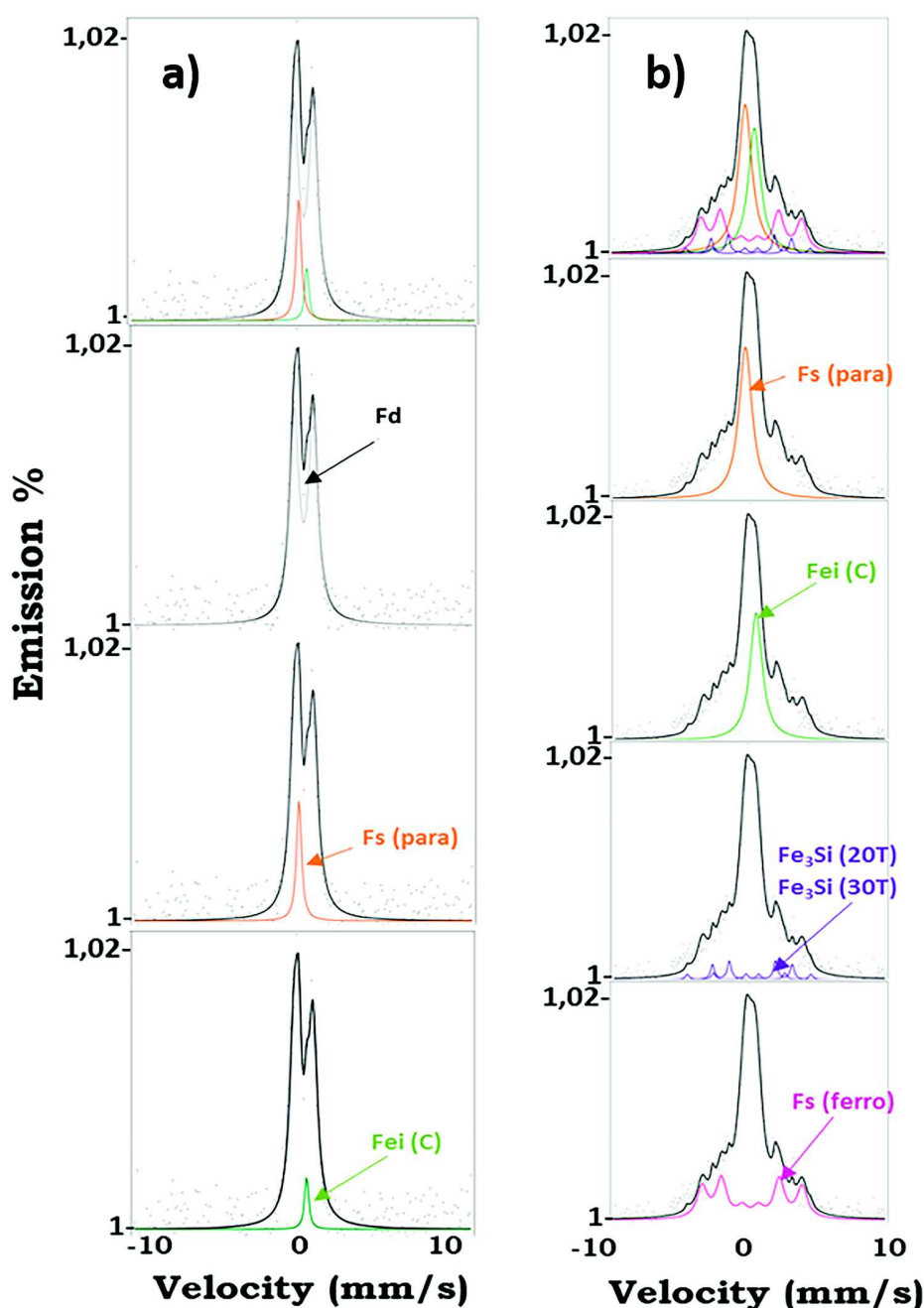


FIG. 4. Mössbauer spectra of the samples implanted at 380 °C with 2 at. % Fe. (a) as-implanted, (b) annealed at 1300 °C.

previously. However, 3 sextuplets, 1 for the contribution called Fs (ferro) and 2 for the  $\text{Fe}_3\text{Si}$  phase were added because of the magnetic behavior of this sample and the presence of small nano-particles with an  $\text{Fe}_3\text{Si}$  core phase. The Fe (ferro) sextet is considered as the magnetic fraction of diluted Fe atoms in the SiC matrix. The  $\text{Fe}_3\text{Si}$  structure known to be ferromagnetic is represented by the second and third sextuplets with their characteristic hyperfine fields. The set of fits parameters is presented in Table III.

The different areas of the Mössbauer components indicate that about 37% of Fe atoms are contained in ferromagnetic components [ $\text{Fe}_3\text{Si}$  and Fs (ferro)]. Increasing the annealing temperature of the sample from as-implanted to 1300 °C allowed for increasing the ferromagnetic fraction from 0% to 37%, approximately. This increase is due to the emergency of the Fe diluted in the matrix but also to a small quantity of Fe atoms contained in  $\text{Fe}_3\text{Si}$  core phase nanoparticles. It is very interesting to remark here for this sample that the Fs (ferro) component is much larger (30.18%) than the two components associated with the  $\text{Fe}_3\text{Si}$  phase ( $5.42 + 1.94 = 7.36\%$ ), which is not the case for the samples implanted at 550 °C with 6 at. % Fe. It can also be added that it is this sample which contains the smallest amount of nanoparticles (not showed here). All this is in total agreement with Refs. 13 and 24 in which it is said that for a possible DMS system, consisting of Fe-implanted SiC, the maximum Fe concentration has to be kept in the 1%–3% range.

#### IV. CONCLUSION

Fe-implanted 6H-SiC samples have been investigated by Mössbauer spectrometry versus the Fe implantation temperature and the annealing temperature allowing for deducing the Fe fractions entering the interstitial and substitutional sites of this structure. For the 380 °C as implanted state sample, the Mössbauer spectrum presents an Fd component (much larger than the two other components) which is characteristic of a strongly disturbed state, often called “amorphous state.” The spectrum of the 550 °C implanted sample does not present this Fd component, which means that the 6H-SiC structure has been restored for this temperature. Above 550 °C, the Fe atoms are shared in the 6H-SiC structure only between Si substitution sites (Fs (para) and Fs (ferro) components) and C interstitial sites (Fei C

component). Moreover, in the majority of samples, Fe rich nanoparticles are observed. The quantity and the size of these nanoparticles depend on the implantation and annealing temperatures but their presence is detrimental to obtaining a DMS. Thanks to a previous tomographic atom probe study, we could determine the samples which contain the smallest amount of nanoparticles and this study allowed us to determine all the ferromagnetic components of the samples and particularly the components due to diluted Fe atoms. As observed above in the study of the Mössbauer spectra, it is the sample implanted at 380 °C with 2 at. % Fe and annealed at 1300 °C that seems to suit the intended properties best. The implanted Fe atom amount, relatively low, and the 380 °C implantation temperature, the smallest of the 2 implantation temperatures, allows for avoiding or at least limiting the formation of nanoparticles. The annealing at 1300 °C allows for revealing the magnetism of this sample. It is likely that by optimizing these two parameters, one could tend towards a diluted and magnetic semiconductor based on 6H-SiC.

#### ACKNOWLEDGMENTS

This work was supervised by the MAGMA project funded by Region of Normandy and the European Regional Development Fund of Normandy (ERDF).

- <sup>1</sup>T. Dietl, K. Sato, T. Fukushima, A. Bonanni, M. Jamet, A. Barski, S. Kuroda, M. Tanaka, P. N. Hai, H. Katayama-Yoshida *et al.*, *Rev. Mod. Phys.* **87**, 1311 (2015).
- <sup>2</sup>H. Munekata, H. Ohno, S. von Molnar, A. Segmuller, L. L. Chang, and L. Esaki, *Phys. Rev. Lett.* **63**, 1849 (1989).
- <sup>3</sup>H. Ohno, A. Chen, F. Matsukura, A. Oiwa, A. Endo, S. Katsumoto, and Y. Iye, *Appl. Phys. Lett.* **69**, 363 (1996).
- <sup>4</sup>F. Matsukura, H. Ohno, A. Shen, and Y. Sugawara, *Phys. Rev. B* **57**, R2037(R) (1998).
- <sup>5</sup>D. Chida, K. Takamura, F. Matsukura, and H. Ohno, *Appl. Phys. Lett.* **82**, 3020 (2003).
- <sup>6</sup>K. Olejnik, M. Owen, V. Novák, J. Mašek, A. Irvine, J. Wunderlich, and T. Jungwirth, *Phys. Rev. B* **78**, 054403 (2008).
- <sup>7</sup>T. Dietl, H. Ohno, and F. Matsukura, *Phys. Rev. B* **63**, 195205 (2001).
- <sup>8</sup>A. Bonanni and T. Dietl, *Chem. Soc. Rev.* **39**, 528 (2010).
- <sup>9</sup>A. V. Los, A. N. Timoshevskii, V. E. Los, and S. A. Kalkuta, *Phys. Rev. B* **76**, 165204 (2007).
- <sup>10</sup>G. Bouzerar and R. Bouzerar, *C. R. Phys.* **16**, 731 (2015).
- <sup>11</sup>N. Theodoropoulou, A. F. Hebard, S. N. G. Chu, M. E. Overberg, C. R. Abernathy, S. J. Pearton, R. G. Wilson, and J. M. Zavada, *Electrochem. Solid-State Lett.* **4**, G119 (2001).
- <sup>12</sup>S. J. Pearton, K. P. Lee, M. E. Overberg, C. R. Abernathy, N. Theodoropoulou, A. F. Hebard, R. G. Wilson, S. N. G. Chu, and J. Zavada, *J. Electron. Mater.* **31**, 336 (2002).
- <sup>13</sup>F. Stromberg, W. Keune, X. Chen, S. Bedanta, H. Reuther, and A. Mücklich, *J. Phys.: Condens. Matter* **18**, 9881 (2006).
- <sup>14</sup>C. Dupeyrat, A. Declémy, M. Drouet, D. Eyidi, L. Thomé, A. Debelle, M. Viret, and F. Ott, *Phys. B* **404**, 4731 (2009).
- <sup>15</sup>M. L. Diallo, L. Lechevallier, A. Fnidiki, R. Lardé, A. Debelle, L. Thomé, M. Viret, M. Marteau, D. Eyidi, A. Declémy, F. Cuvilly, and I. Blum, *J. App. Phys.* **117**, 183907 (2015).
- <sup>16</sup>M. L. Diallo, A. Fnidiki, M. Viret, M. Drouet, D. Eyidi, and A. Declémy, *Phys. Status Solidi C* **12**, 60 (2015).
- <sup>17</sup>A. Declémy, A. Debelle, C. Dupeyrat, L. Thomé, I. Monnet, and D. Eyidi, *Appl. Phys. A* **106**, 679 (2012).
- <sup>18</sup>W. J. Weber, L. M. Wang, N. Yu, and N. J. Hess, *Mater. Sci. Eng. A* **253**(1-2), 62 (1998).
- <sup>19</sup>A. Fnidiki, F. Richomme, J. Teillet, F. Pierre, P. Boher, and P. Houday, *J. Magn. Magn. Mater.* **121**, 520 (1993).
- <sup>20</sup>J. P. Eymery, A. Fnidiki, and J. P. Riviere, *Nucl. Instrum. Methods* **209/210**, 919 (1983).

TABLE III. Mössbauer parameters used to fit the samples implanted at 380 °C with 2 at. % Fe.

Samples	Components	$\delta$ (mm/s)	QS (mm/s)	$B_{\text{hf}}$ (kOe)	Relative area (%)
As-implanted	Fd	-0.04	1.193		82
	Fs (para)	-0.27	0		13
	Fei (C)	0.24			5
Annealed 1300 °C	Fs (para)	-0.25			35.02
	Fei (C)	0.48			27.43
	Fs (ferro)	0.16		246	30.18
	$\text{Fe}_3\text{Si}$	0.235		196	5.42
		0.021		304	1.94



- <sup>21</sup>H. P. Gunnlaugsson, K. Bharuth-Ram, M. Dietrich, M. Fanciulli, H. O. U. Fynbo, and G. Weyer, *Hyperfine Interact.* **169**, 1319 (2006).
- <sup>22</sup>A. Los and V. Los, *J. Phys.: Condens. Matter* **21**, 206004 (2009).
- <sup>23</sup>M. S. Miao and W. R. L. Lambrecht, *Phys. Rev. B* **68**, 125204 (2003).
- <sup>24</sup>V. L. Shaposhnikov and N. A. Sobolev, *J. Phys.: Condens. Matter* **16**, 1761 (2004).
- <sup>25</sup>M. L. Diallo, Thèse de Doctorat de l'Université de Rouen, 2017.
- <sup>26</sup>J. Lefevre, Thèse de Doctorat de l'École Polytechnique, Palaiseau, France, 2008.